Hadronic production of W and Z bosons at large transverse momentum

Edmond L. Berger,[1] Jun Gao,[1] Zhong-Bo Kang,[2] Jian-Wei Qiu,[3,4] and Hao Zhang[5]

[1]*High Energy Physics Division, Argonne National Laboratory, Argonne, Illinois 60439, USA*
[2]*Theoretical Division, Los Alamos National Laboratory, Los Alamos, New Mexico 87545, USA*
[3]*Physics Department, Brookhaven National Laboratory, Upton, New York 11973-5000, USA*
[4]*C.N. Yang Institute for Theoretical Physics and Department of Physics and Astronomy, Stony Brook University, Stony Brook, New York 11794-3840, USA*
[5]*Department of Physics, University of California, Santa Barbara, California 93106, USA*

(Received 2 April 2015; published 2 June 2015)

We introduce a modified factorization formalism in quantum chromodynamics for hadronic production of W and Z bosons at large transverse momentum p_T. When p_T is much larger than the invariant mass Q of the vector boson, this new factorization formalism systematically resums the large fragmentation logarithms, $\alpha_s^m \ln^m(p_T^2/Q^2)$, to all orders in the strong coupling α_s. Using our modified factorization formalism, we present the next-to-leading-order (NLO) predictions for W and Z boson production at high p_T at the CERN Large Hadron Collider and at a future 100 TeV proton-proton collider. Our NLO results are about 5% larger in normalization, and they show improved convergence and moderate reduction of the scale variation compared to the NLO predictions derived in a conventional fixed-order perturbative expansion.

DOI: 10.1103/PhysRevD.91.113001 PACS numbers: 14.70.Fm, 12.38.Bx, 12.38.Cy, 14.70.Hp

I. INTRODUCTION

Successful operation of the CERN Large Hadron Collider (LHC) and associated particle detectors have led to the discovery of the Higgs boson, the final piece of the standard model (SM) [1,2] of particle physics, along with the exploration of strong interaction short-distance phenomena in high-energy processes at much greater values of the production transverse momentum. Future experimental investigations, at higher collision energy and with greater luminosity, promise refined understanding of the nature of electroweak symmetry breaking and possible evidence of new physics beyond the SM. Some of these searches will focus on deviations from SM expectations or on anomalies in high-energy tails of various kinematic distributions. Precise SM predictions for these observables and distributions are important assets for discovery of new physics.

The production distributions of massive electroweak (EW) gauge bosons, W's and Z's, are among observables that can be sensitive to physics beyond the SM, either because new states in extensions of the SM may decay into W and Z bosons or because the lepton distributions from SM W and Z decay are important backgrounds for high-energy lepton signatures in new physics models. The leptons could mimic the signature of boosted objects from the decay of a new heavy resonance. Moreover, W and Z boson production serve as tests of perturbative QCD calculations, and data on their distributions are important in the determination of the parton distribution functions (PDFs) [3]. Among measurements of W and Z production, precise cross sections at large transverse momentum hold particular interest. The SM Z boson production at large p_T can be used for jet energy-scale calibration. Existing studies show the possibility of using W and Z boson production at large p_T to further constrain the gluon PDFs [4,5]. Transverse momentum distributions of W and Z bosons have been measured at the LHC [6,7] but with relatively large uncertainties.

To exploit the full potential of the data, ever more precise SM predictions are needed, requiring better understanding of the size of high-order perturbative corrections. The p_T spectra of W and Z boson production in hadronic collisions have been calculated perturbatively in the SM. The leading-order (LO) cross section at a finite p_T is of $\mathcal{O}(\alpha_{em}\alpha_s)$. The next-to-leading-order (NLO) QCD corrections were calculated decades ago [8–10] and found to be sizable for the energy of the LHC. The EW corrections were studied extensively in recent years [11–18]. The W and Z production at small $p_T \ll Q$ ($\sim$mass of W or Z) has received a lot of attention in connection with the resummation of the effects Sudakov double logarithms in QCD [19–33], also important for precise measurements of the W boson mass in hadronic collisions. Improved predictions are awaited of W and Z production at large p_T beyond NLO corrections [34–41]. Work is in progress on the full next-to-next-to-leading-order (NNLO) QCD corrections to the p_T spectrum of W and Z production, similar to the case of Higgs boson production [42,43].[1]

In this paper, we explore another approach to theoretical improvement by identifying potentially large QCD

[1]After our paper was submitted, the NNLO QCD corrections to W + jet production appeared [44].

logarithms from high-order perturbative calculations and resumming these logarithms to all orders. QCD corrections to the short-distance partonic scattering cross sections of W and Z production at large p_T could receive one power of a large logarithm, $\ln(p_T^2/Q^2)$, for every additional power of α_s. Such large logarithms come from partonic subprocesses in which the high p_T heavy boson is radiated from a more energetic quark (or a parton in general), as is illustrated in Fig. 1. For the production of EW gauge bosons with mass $Q \sim 100$ GeV, the fragmentation logarithm, $\ln(p_T^2/Q^2) \sim 4.6$, when the boson's transverse momentum $p_T \sim 1$ TeV, and could be a potential source of large high-order corrections.

The leading contribution from the fragmentation logarithm of the diagrams in Fig. 1 has the approximate form

$$\hat{\sigma}^F/\hat{\sigma}_f^{\mathrm{LO}} \sim \frac{\alpha_s(\mu)}{2\pi} P_{f\to q}(z) \int_{k_{\min}^2}^{k_{\max}^2} \frac{dk^2}{k^2} \sim \frac{\alpha_s(\mu)}{2\pi} \ln\left(\frac{p_T^2}{Q^2}\right), \tag{1}$$

where $\hat{\sigma}_f^{\mathrm{LO}}$, with parton flavor $f = q, g$, represents the lower-order contribution to the production cross section without the quark to quark-gluon (or gluon to quark-antiquark) splitting in Fig. 1 and $P_{f\to q}(z)$ is the LO splitting function for a parton of flavor f to fragment into a quark, e.g., $P_{g\to q}(z) = (1/2)[z^2 + (1-z)^2]$ with the color factor $1/2$. To obtain the second line in Eq. (1), we use the fact that the fragmentation contribution is dominated by the large z region and the size of the LO splitting functions to a quark at large z is of $\mathcal{O}(1)$. Since the factorization scale could be chosen from $\mathcal{O}(Q)$ to $\mathcal{O}(p_T)$, we could estimate the size of the high-order corrections from the LO fragmentation logarithms as

$$\frac{\alpha_s(\mu)}{2\pi} \ln\left(\frac{p_T^2}{Q^2}\right) \lesssim \frac{\alpha_s(Q)}{2\pi} \ln\left(\frac{p_T^2}{Q^2}\right) \lesssim 10\%, \tag{2}$$

for $p_T \sim 1$ TeV. That is, the higher-order corrections from the fragmentation logarithms to the production of heavy EW gauge boson of mass $Q \sim 100$ GeV, $[(\alpha_s(\mu)/2\pi)\ln(p_T^2/Q^2)]^m$ with $m > 1$, should be under control perturbatively. It was pointed out in Ref. [45] that the double logarithms from radiation of soft Z bosons can induce large higher-order corrections in the large jet p_T region of $Z +$ jets production. This situation is different from the case studied here where we are looking at inclusive Z boson production at large p_T. The double logarithms are highly suppressed in our case.

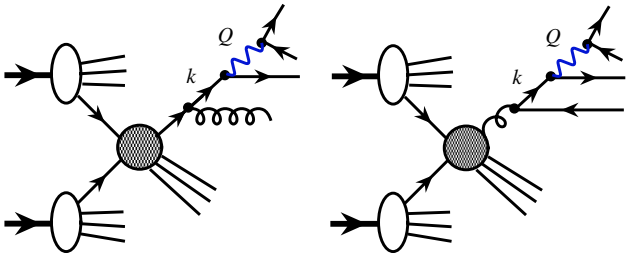

FIG. 1 (color online). Leading-order QCD diagrams that lead to the fragmentation logarithms in W and Z production. The diagram on the left (right) provides the fragmentation logarithm from quark (gluon) splitting.

In this paper, we use a modified QCD factorization formalism for calculating the hadronic cross sections of W and Z production at large transverse momentum p_T. This formalism is similar to the one that we introduced for the low mass Drell–Yan cross section at large p_T in previous work [46–48]. To resum the $\alpha_s^m \ln^m(p_T^2/Q^2)$-type large logarithms, we reorganize the conventional fixed-order perturbative expansion of W and Z cross sections at large p_T into factored "direct" and "fragmentation" contributions, as demonstrated in Sec. II:

$$\frac{d\sigma_{AB\to V(Q)X}}{dp_T^2 dy} \equiv \frac{d\sigma_{AB\to V(Q)X}^{\mathrm{Dir}}}{dp_T^2 dy} + \frac{d\sigma_{AB\to V(Q)X}^{\mathrm{Frag}}}{dp_T^2 dy}.$$

All powers of the logarithmic $\alpha_s \ln(p_T^2/Q^2)$ high-order corrections are completely resummed into W and Z fragmentation functions and included into the fragmentation contributions, while the short-distance partonic hard parts for both direct and fragmentation contributions are free of the large logarithms and can be systematically calculated order by order in powers of α_s. Using our modified factorization scheme, we calculate the NLO predictions for W and Z boson production at high p_T at LHC energies, as well as at a future 100 TeV proton-proton collider. The perturbatively calculated W and Z cross sections at large p_T show improved convergence, as well as moderate reduction of the scale variations compared to the conventional NLO perturbative expansion.

The situation in W and Z production is very different from the fragmentation contributions to light hadron production, where the logarithms could run into the nonperturbative region, and also numerically different from the role of fragmentation contributions to the production of low mass Drell–Yan pairs or heavy quarkonia at high p_T [47,49]. The key difference is the mass of the heavy EW gauge bosons. To produce heavy EW gauge bosons of mass Q, as shown in Fig. 1, the invariant mass of the fragmenting parton of momentum k should be sufficiently large, as $\sqrt{k^2} \gtrsim Q$. Consequently, the radiation from the fragmenting parton is similar to the radiation from a heavy quark of mass $\sqrt{k^2} \gtrsim Q$ and is strongly suppressed for the phase space within the angle, $\sqrt{k^2}/k_0$, of the fragmenting parton, the so-called "dead-cone" effect [50]. In addition to the much smaller phase space for the radiation, the large virtuality of the fragmenting parton also sets the

renormalization scale μ for the strong coupling constant $\alpha_s(\mu) \lesssim \alpha_s(M_Z) \sim 0.118$ with Z mass, M_Z. With the current limit of collision energies, it is the combination of small α_s and the restricted phase space for the radiation that controls the size of the corrections from high-order fragmentation logarithms. In this paper, we verify this conclusion by performing explicit all-order resummation of the fragmentation logarithms.

The rest of our paper is organized as follows. In Sec. II, we introduce our modified factorization scheme for EW gauge boson production at large p_T and compare it with the conventional fixed-order perturbative expansion scheme. In Sec. III, applying our modified factorization scheme, we present our predictions for the W and Z fragmentation functions, as well as our calculations of the LO and NLO cross sections of W and Z production at large p_T at LHC energies and at a $\sqrt{s} = 100$ TeV future proton-proton collider. We also discuss the improvement of our modified factorization formalism over the conventional fixed-order perturbative expansion. Our summary and conclusions are presented in Sec. IV.

II. QCD FACTORIZATION OF VECTOR BOSON PRODUCTION AT LARGE p_T

The cross section for producing an on-shell EW gauge boson of momentum p^μ can be factored systematically in QCD perturbation theory as [51]

$$\frac{d\sigma_{AB\to V(Q)X}}{dp_T^2 dy} = \sum_{a,b} \int dx_1 f_a^A(x_1,\mu) \int dx_2 f_b^B(x_2,\mu) \times \frac{d\hat{\sigma}^{\rm Pert}_{ab\to V(Q)X}}{dp_T^2 dy}(x_1,x_2,Q,p_T,y;\mu), \quad (3)$$

under the usual assumption that the physically measured quantities Q and p_T are both much larger than $\Lambda_{\rm QCD}$. In Eq. (3), the variables Q, p_T, and y are the mass, transverse momentum, and rapidity of the vector boson, respectively; the symbol X stands for an inclusive sum over final states that recoil against the observed vector boson. The sum $\sum_{a,b}$ runs over all parton flavors, and f_a^A and f_b^B are the corresponding PDFs, with the partons' momentum fractions x_1 and x_2, respectively; μ represents the renormalization and factorization scale, which is of the order of the energy exchange of the hard collision: $\mu \sim \sqrt{Q^2 + p_T^2}$. The function $d\hat{\sigma}^{\rm Pert}_{ab\to V(Q)X}/dp_T^2 dy$ in Eq. (3) is the short-distance hard part of the partonic scattering cross section. It can be calculated in perturbation theory in powers of the QCD coupling $\alpha_s(\mu)$. The first two terms of the perturbative expansion, $d\hat{\sigma}^{\rm C\text{-}LO}$ and $d\hat{\sigma}^{\rm C\text{-}NLO}$, including perturbative contributions up to $\mathcal{O}(\alpha_{em}\alpha_s)$ and $\mathcal{O}(\alpha_{em}\alpha_s^2)$, respectively, have been available in the literature for sometime [8–10]. The superscript "C" indicates the *conventional* fixed-order perturbative expansion.

Beyond the leading order in α_s, when $p_T \gg Q$, the perturbative functions $d\hat{\sigma}^{\rm Pert}_{ab\to V(Q)X}/dp_T^2 dy$ in Eq. (3) can receive large high-order corrections in powers of $\alpha_s \ln(p_T^2/Q^2)$ arising from the radiation of partons along the direction of the observed vector boson. Such large logarithmic corrections can be systematically resummed into the parton to vector-boson fragmentation functions, $D_{f\to V}$, as demonstrated for the case of the virtual photon [47]. The perturbative series for $d\hat{\sigma}^{\rm Pert}_{ab\to V(Q)X}/dp_T^2 dy$ can therefore be reorganized into two terms as in Ref. [47],

$$\frac{d\hat{\sigma}^{\rm Pert}_{ab\to V(Q)X}}{dp_T^2 dy}(x_1,x_2,Q,p_T,y;\mu) = \frac{d\hat{\sigma}^{\rm Dir}_{ab\to V(Q)X}}{dp_T^2 dy}(x_1,x_2,Q,p_T,y;\mu,\mu_D) + \frac{d\hat{\sigma}^{\rm Frag}_{ab\to V(Q)X}}{dp_T^2 dy}(x_1,x_2,Q,p_T,y;\mu,\mu_D), \quad (4)$$

where the superscripts "Dir" and "Frag" represent the direct and the fragmentation contributions, respectively. The latter includes the perturbative fragmentation logarithms, and it can be further factored as [52]

$$\frac{d\hat{\sigma}^{\rm Frag}_{ab\to V(Q)X}}{dp_T^2 dy} = \sum_c \int \frac{dz}{z^2}\left[\frac{d\hat{\sigma}_{ab\to cX}}{dp_{cT}^2 dy}(x_1,x_2,p_c;\mu_D)\right] \times D_{c\to V}(z,\mu_D^2;Q^2), \quad (5)$$

where $p_c^\mu = \hat{p}^\mu/z$, with $\hat{p}^\mu$ defined to be p^μ at $Q^2 = 0$, corresponding to the approximation $Q^2 \ll p_T^2$ made for $d\hat{\sigma}_{ab\to cX}/dp_{cT}^2 dy$ in Eq. (5), which is a short-distance hard part for partons of flavors a and b to produce a parton of flavor c and momentum p_c. The fragmentation scale $\mu_D \sim p_T$ is introduced to separate the direct and fragmentation contributions in Eq. (4), and its dependence would be cancelled if both contributions include all-order corrections [47].

The fragmentation contribution in Eq. (5) shares the typical two-stage generic pattern of the fragmentation production of a single particle at large transverse momentum p_T (much larger than its mass): the production of an on-shell parton of flavor c at the distance scale $1/p_T$, convoluted with a fragmentation function that includes the leading logarithmic contributions from the "running" of the distance scale from $1/\mu_D \sim 1/p_T$ to $1/\mu_{D0} \sim 1/Q$. When $Q \gg \Lambda_{\rm QCD}$, which is the case for the W and Z boson, the parton to vector-boson fragmentation function $D_{f\to V}$ is perturbative, and so is the whole resummed fragmentation contribution, $\hat{\sigma}^{\rm Frag}$ in Eq. (5) [47].

The direct contribution in Eq. (4) is perturbatively calculable in a power series of α_s [47], and it is defined as

$$\frac{d\hat{\sigma}^{\rm Dir}_{ab\to V(Q)X}}{dp_T^2 dy} \equiv \frac{d\hat{\sigma}^{\rm Pert}_{ab\to V(Q)X}}{dp_T^2 dy} - \frac{d\hat{\sigma}^{\text{F-Asym}}_{ab\to V(Q)X}}{dp_T^2 dy}, \tag{6}$$

where $d\hat{\sigma}^{\rm Pert}$ is the conventional fixed-order perturbative QCD calculation. Moreover, $d\hat{\sigma}^{\text{F-Asym}}$, with the superscript "Asym" referring to an "asymptotic" contribution, is simply the perturbative expansion of the resumed fragmentation contribution, $d\hat{\sigma}^{\rm Frag}$ in Eq. (5), to the same order in powers of α_s as $d\hat{\sigma}^{\rm Pert}$ in Eq. (6). It is effectively a subtraction term to systematically remove from $d\hat{\sigma}^{\rm Pert}$ all fragmentation logarithms which have been resummed into the fragmentation contribution, $d\hat{\sigma}^{\rm Frag}$ in Eq. (5). The subtraction avoids double counting order by order in powers of α_s. Consequently, the direct contribution is free of the large fragmentation logarithms, while it still keeps all nonlogarithmic terms from the physics between the scales p_T and Q. Note that $d\hat{\sigma}^{\text{Dir-LO}} = d\hat{\sigma}^{\text{C-LO}}$ since the fragmentation contributions start at $\mathcal{O}(\alpha_{em}\alpha_s^2)$.

By substituting Eqs. (4) and (5) into Eq. (3), we obtain our modified factorization formalism for heavy EW vector boson production in hadronic collisions,

$$\frac{d\sigma_{AB\to V(Q)X}}{dp_T^2 dy} \equiv \frac{d\sigma^{\rm Dir}_{AB\to V(Q)X}}{dp_T^2 dy} + \frac{d\sigma^{\rm Frag}_{AB\to V(Q)X}}{dp_T^2 dy}, \tag{7}$$

where $d\sigma^{\rm Dir}$ is factored in the same way as $d\sigma$ in Eq. (3) with $d\hat{\sigma}^{\rm Pert}$ replaced by $d\hat{\sigma}^{\rm Dir}$ defined in Eq. (6), and $d\sigma^{\rm Frag}$ is

$$\begin{aligned}\frac{d\sigma^{\rm Frag}_{AB\to V(Q)X}}{dp_T^2 dy} = \sum_{a,b,c}\int dx_1 f_a^A(x_1,\mu)\int dx_2 f_b^B(x_2,\mu) \\ \times \int \frac{dz}{z^2}\left[\frac{d\hat{\sigma}^{\rm Frag}_{ab\to cX}}{dp_{c_T}^2 dy}(x_1,x_2,p_c;\mu_D)\right] \\ \times D_{c\to V}(z,\mu_D^2;Q^2),\end{aligned} \tag{8}$$

where the fragmentation functions $D_{c\to V}(z,\mu_D^2;Q^2)$ resum all fragmentation logarithms, and $d\hat{\sigma}^{\rm Frag}_{ab\to cX}$ are partonic hart parts for producing an on-shell parton of flavor "c" and momentum p_c^μ, which are independent of the specific vector boson produced. Actually, they are the same as the perturbative coefficient functions for producing a light hadron, such as a pion, and are available for both the LO and NLO in powers of α_s in the literature [53].

The separation between the direct and the fragmentation contribution in Eq. (7) depends on the definition of the parton to vector-boson fragmentation functions. Different definitions of the fragmentation functions correspond to a different scheme to split the conventional fixed-order perturbative expansion into the direct plus fragmentation contributions. A scheme choice for the fragmentation functions should also fix the asymptotic contribution and, correspondingly, the direct contribution. The sum of these two terms in our modified factorization formalism in Eq. (7) should not be very sensitive to the scheme choice.

The key difference between our modified factorization formula in Eq. (7) and the conventional factorization formula in Eq. (3) resides in the way the large logarithmic contributions from final-state parton splitting are handled. Instead of one perturbative series in powers of α_s in the conventional approach, we have two perturbative expansions in our modified factorization formula: one for the direct contribution and one for the fragmentation contribution. All coefficient functions in the new perturbative expansions are free of large logarithms. The large perturbative logarithms in the conventional expansion in powers of α_s are systematically resummed into the fragmentation functions. As a result, the perturbative expansion of the partonic hard parts in our modified factorization approach has better convergence properties than the conventional fixed-order expansion. In addition, because of the reorganization and resummation of the logarithms, both the LO and NLO cross sections in our new approach include a tower of logarithmically enhanced high-order corrections from the conventional fixed-order perturbative expansion. For example, for the LO cross section, with the lowest-order partonic hard parts retained, the difference between our modified approach in Eq. (7) and the conventional fixed-order approach in Eq. (3) is

$$\begin{aligned}&\sum_{a,b}\int dx_1 f_a^A\int dx_2 f_b^B\left\{\left[\frac{d\hat{\sigma}^{\text{D-LO}}_{ab\to V(Q)X}}{dp_T^2 dy} - \frac{d\hat{\sigma}^{\text{C-LO}}_{ab\to V(Q)X}}{dp_T^2 dy}\right]\right. \\ &\quad\left.+\sum_c\int\frac{dz}{z^2}\frac{d\hat{\sigma}^{\text{F-LO}}_{ab\to cX}}{dp_{c_T}^2 dy}D_{c\to V(Q)}\right\} \\ &=\sum_{a,b,c}\int dx_1 f_a^A\int dx_2 f_b^B\int\frac{dz}{z^2}\frac{d\hat{\sigma}^{\text{F-LO}}_{ab\to cX}}{dp_{c_T}^2 dy}D_{c\to V(Q)},\end{aligned} \tag{9}$$

where the LO relation, $d\hat{\sigma}^{\text{Dir-LO}} = d\hat{\sigma}^{\text{C-LO}}$, is used. Similarly, at NLO, the difference is

$$\begin{aligned}&\sum_{a,b}\int dx_1 f_a^A\int dx_2 f_b^B\left\{\left[\frac{d\hat{\sigma}^{\text{D-NLO}}_{ab\to V(Q)X}}{dp_T^2 dy} - \frac{d\hat{\sigma}^{\text{C-NLO}}_{ab\to V(Q)X}}{dp_T^2 dy}\right]\right. \\ &\quad\left.+\sum_c\int\frac{dz}{z^2}\frac{d\hat{\sigma}^{\text{F-NLO}}_{ab\to cX}}{dp_{c_T}^2 dy}D_{c\to V(Q)}\right\} \\ &=\sum_{a,b,c}\int dx_1 f_a^A\int dx_2 f_b^B\int\frac{dz}{z^2} \\ &\quad\times\left\{\frac{d\hat{\sigma}^{\text{F-LO}}_{ab\to cX}}{dp_{c_T}^2 dy}[D_{c\to V(Q)} - D^{(0)}_{c\to V(Q)}]\right. \\ &\quad\left.+\left[\frac{d\hat{\sigma}^{\text{F-NLO}}_{ab\to cX}}{dp_{c_T}^2 dy} - \frac{d\hat{\sigma}^{\text{F-LO}}_{ab\to cX}}{dp_{c_T}^2 dy}\right]D_{c\to V(Q)}\right\}.\end{aligned} \tag{10}$$

In deriving Eq. (10), we use the definition in Eq. (6) and the relation

$$\frac{d\hat{\sigma}^{\text{F-Asym-NLO}}_{ab\to V(Q)X}}{dp_T^2 dy} = \sum_c \int \frac{dz}{z^2} \frac{d\hat{\sigma}^{\text{F-LO}}_{ab\to cX}}{dp_{cT}^2 dy} D^{(0)}_{c\to V(Q)}, \tag{11}$$

where $D^{(0)}_{c\to V(Q)}$ is the fragmentation function for a single parton of flavor c to fragment into a vector boson of invariant mass Q, expanded perturbatively to $\mathcal{O}(\alpha_{em}\alpha_s^0)$.

In comparison with a conventional fixed-order calculation at the same orders, Eqs. (9) and (10) show that our modified factorization formalism in Eq. (7) includes the all-orders resummation of final-state fragmentation logarithms, plus additional short-distance high-order contributions. The first term on the right-hand side of Eq. (10) comes from the resummation of leading logarithms to all orders, and the second term is from the $\mathcal{O}(\alpha_s^3)$ corrections to the partonic hard parts. To the order in which we work, the full correction is the sum of the two. In our presentation of numerical results in Sec. III, the sum of the two terms in Eq. (10) is referred to as the type-B correction to the NLO term of the conventional fixed-order perturbative calculation, while the first term alone is denoted the type-A correction.

The resummation of the fragmentation logarithms into the single parton to vector-boson fragmentation functions is achieved by solving the inhomogeneous evolution equations [52],

$$\begin{aligned}\mu_D^2 \frac{d}{d\mu_D^2} D_{c\to V}(z,\mu_D^2;Q^2) &= \left(\frac{\alpha_{\text{em}}}{2\pi}\right)\gamma_{c\to V}(z,\mu_D^2,\alpha_s;Q^2) \\ &+ \left(\frac{\alpha_s}{2\pi}\right)\sum_d \int_z^1 \frac{dz'}{z'} P_{c\to d}\left(\frac{z}{z'},\alpha_s\right) D_{d\to V}(z',\mu_D^2;Q^2),\end{aligned} \tag{12}$$

where $c,d = q,\bar{q},g$. The ambiguity in defining the fragmentation function is connected to the renormalization of its perturbative UV divergence and the choice of the fragmentation scale, μ_D. In Eq. (12), the evolution kernels $P_{c\to d}$ are IR safe, evaluated at a single hard scale, μ_D, and calculated perturbatively as a power series in α_s. These kernels are insensitive to the specific vector meson produced and are the same as the evolution kernels for pion or other light hadron fragmentation functions. They are the same as the splitting functions of the Dokshitzer–Gribov–Lipatov–Altarelli–Parisi evolution equations [54] at the leading order.

The inhomogeneous term in the evolution equations can also be calculated perturbatively, and in general it has power correction terms of the form Q^2/μ_D^2, owing to the mass of the vector boson, and therefore it depends on the nature of the vector boson produced. In the invariant mass cutoff scheme [52,55], the lowest-order quark-to-virtual photon evolution kernel $\gamma^{(0)}_{q\to\gamma^*}$ was derived in Ref. [52]. With a simple generalization, we compute the inhomogeneous evolution kernel for a quark to fragment into an EW gauge boson of invariant mass Q, $\gamma^{(0)}_{q\to V}$, and we obtain

$$\gamma^{(0)}_{q\to V}(z,k^2;Q^2) = \frac{(|g_L^{Vq}|^2+|g_R^{Vq}|^2)}{2}\left[\frac{1+(1-z)^2}{z} - z\left(\frac{Q^2}{zk^2}\right)\right]\theta\left(k^2-\frac{Q^2}{z}\right), \tag{13}$$

where k^2 is the invariant mass of the parent quark and is identified as μ_D^2, and the θ-function is a consequence of the mass threshold. Here, $g_{L,R}^{Vq}$ are the EW couplings between quarks and the EW gauge bosons, with $\{g_L^{Wq}, g_R^{Wq}\} = \{1/(\sqrt{2}s_w), 0\}$ for the W boson, and $\{g_L^{Zq}, g_R^{Zq}\} = \{(1/2 - 2s_w^2/3)/(s_w c_w), -2s_w/(3c_w)\}$ and $\{(-1/2 + s_w^2/3)/(s_w c_w), +s_w/(3c_w)\}$ for the Z boson to couple to the up- and down-type quarks, respectively. We us s_w and c_w to represent the sine and cosine of the weak-mixing angle. The gluon to vector-boson evolution kernel vanishes at the lowest order,

$$\gamma^{(0)}_{g\to V}(z,k^2;Q^2) = 0, \tag{14}$$

because the gluon does not interact directly with the EW gauge bosons.

The choice of factorization scheme is not unique. We use the invariant mass cutoff scheme [52,55]. Some choices, such as the modified minimum subtraction ($\overline{\text{MS}}$) scheme, may not respect the mass threshold when $Q^2 \neq 0$ and lead to negative fragmentation functions [52,55]. QCD corrections to the lowest-order parton to vector-boson splitting function $\gamma^{(0)}_{c\to V}$ can be evaluated in principle order by order in α_s.

If $Q \gg \Lambda_{\text{QCD}}$, the parton to vector-boson fragmentation functions are completely perturbative, as is the case for our study here. The lowest-order parton to vector-boson fragmentation functions are

$$D^{(0)}_{q\to V}(z,\mu_D^2;Q^2) = \frac{(|g_L^{Vq}|^2+|g_R^{Vq}|^2)}{2}\left(\frac{\alpha_{em}}{2\pi}\right) \times \left[\frac{1+(1-z)^2}{z}\ln\left(\frac{z\mu_D^2}{Q^2}\right) - z\left(1-\frac{Q^2}{z\mu_D^2}\right)\right], \tag{15}$$

$$D^{(0)}_{g\to V}(z,\mu_D^2;Q^2) = 0. \tag{16}$$

We must specify a boundary condition in order to solve the evolution equations in Eq. (12). A natural boundary condition following the mass threshold constraint is [47,52]

$$D_{c\to V}(z,\mu_D^2 \le Q^2/z;Q^2) = 0, \tag{17}$$

for any flavor c, if we choose the invariant mass cutoff scheme for the fragmentation functions.

To conclude this section, we emphasize that our modified factorization formalism in Eq. (4) effectively reorganizes the *single* perturbative expansion of conventional QCD factorization, in Eq. (3), into *two* perturbative expansions in Eq. (7), plus the perturbatively calculated evolution kernels for the fragmentation functions. The main advantage of this reorganization is that the new perturbative expansions are evaluated at a single hard scale and are free of large logarithms. As shown in Sec. III, the ratios of the NLO over the LO contributions in the new perturbative expansions are smaller than the ratios evaluated in the conventional approach.

III. NUMERICAL RESULTS

We present our numerical results in this section. We choose the G_F parametrization scheme [56] for the EW couplings with $M_W = 80.385$ GeV, $M_Z = 91.1876$ GeV, $M_t = 173$ GeV, and $G_F = 1.166379 \times 10^{-5}$ GeV^{-2} [57]. We assume a diagonal Cabibbo–Kobayashi–Maskawa matrix of the SM in the calculation for simplicity. We use META1.0 PDF [58] of the proton, which is a NNLO PDF set that combines information from the CT10 [59], MSTW2008 [60], and NNPDF2.3 [61] PDF sets, and three-loop running of the QCD coupling constants with $N_f = 5$ active quark flavors and $\alpha_s(M_Z) = 0.118$.

A. Fragmentation functions

At LO only quarks can fragment into EW vector bosons, for which the fragmentation functions are proportional to the square of the EW couplings. As seen in Eq. (15), for example, the up-type quark can fragment into a W^+ boson at LO but not into a W^- boson. The fragmentation functions are the same for a quark and antiquark to a virtual-photon or Z boson. Similarly fragmentation functions are equal for up-type quarks to W^+ and down-type quarks to W^-. The gluon can fragment into W or Z bosons only at higher orders through intermediate quarks, and thus the fragmentation functions are suppressed.

In Fig. 2, we show the momentum fraction z dependence of the LO and resummed parton to vector-boson fragmentation functions for the Z and W^+ bosons. In each figure we also plot the parton to virtual-photon fragmentation functions with the same mass. We choose a typical fragmentation scale of 800 GeV and show results for the u quark as an example. The fragmentation functions have a peak in z, a consequence of the vector boson's mass threshold. The height of the peak is proportional to the square of the corresponding EW couplings.

In Fig. 3, we show the resummed corrections to the LO fragmentation functions in percentage. As expected, the resummed contributions increase the fragmentation function at small and moderate z values, while they reduce it for large z values. The observed differences of the fractional corrections for different vector bosons are caused by the difference of their EW couplings through the mixing of singlet and nonsinglet evolutions. We further show the evolution of the fragmentation function for a u quark into a Z boson with momentum fraction $z = 0.04$ in Fig. 4. The scale dependence of the LO fragmentation functions are dominated by the logarithmic term in Eq. (15). The resummed corrections here are always positive.

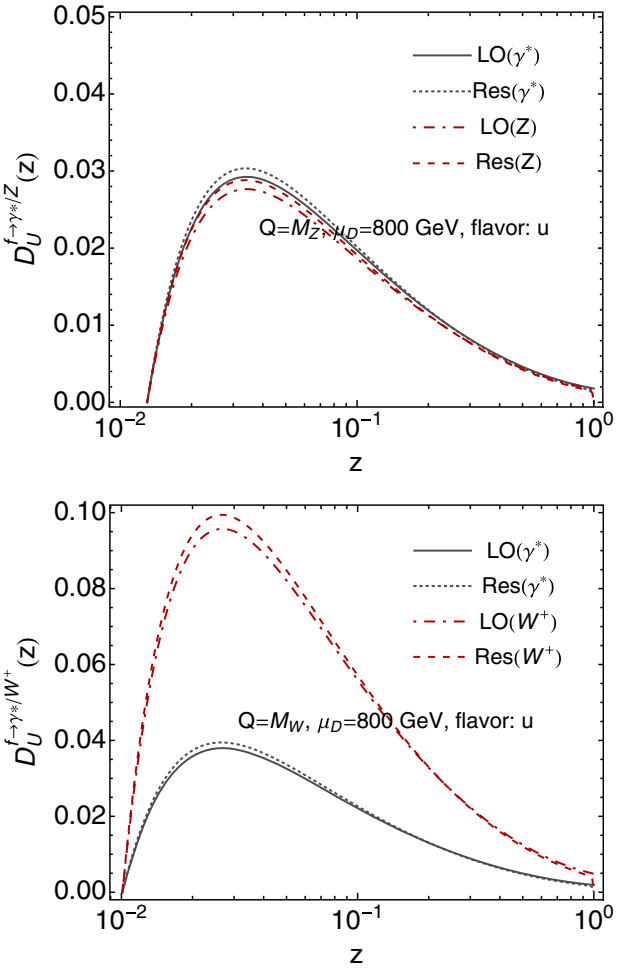

FIG. 2 (color online). The z dependence of the LO and resummed fragmentation functions of a u quark into a Z and a W^+ boson for a fragmentation scale $\mu_D = 800$ GeV. For reference, we also plot the fragmentation function of a virtual photon with the same mass.

B. W and Z boson production at large p_T in the conventional expansion scheme

In this subsection we present the cross sections of W and Z boson production at large p_T at LO and NLO accuracy in the conventional fixed-order perturbative expansion, defined in Eq. (3), based on the analytical results in Refs. [8–10]. We plot in Fig. 5 the p_T dependence of the double-differential cross sections of the vector

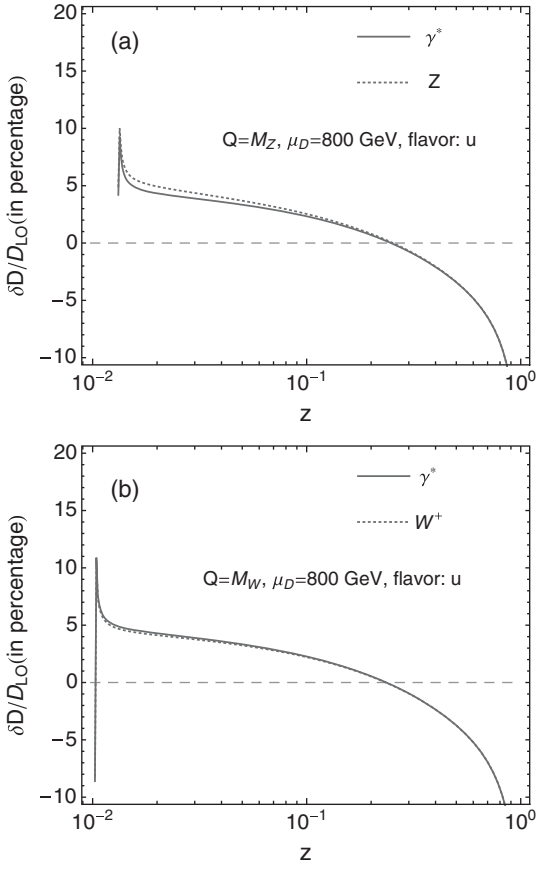

FIG. 3. Percentage change of the resummed to the LO fragmentation functions for a u quark to (a) Z and (b) W^+ boson for a fragmentation scale $\mu_D = 800$ GeV.

bosons at a central rapidity, $y = 0$. We show the results at $\sqrt{s} = 8$ and 14 TeV at the LHC, and at $\sqrt{s} = 100$ TeV at a future proton-proton collider, with increasing range of p_T as allowed by the higher collision energy. We focus on the large p_T region (> 500 GeV) where the perturbative logarithms, $\propto \ln(p_T/Q)$, are large. We set the factorization

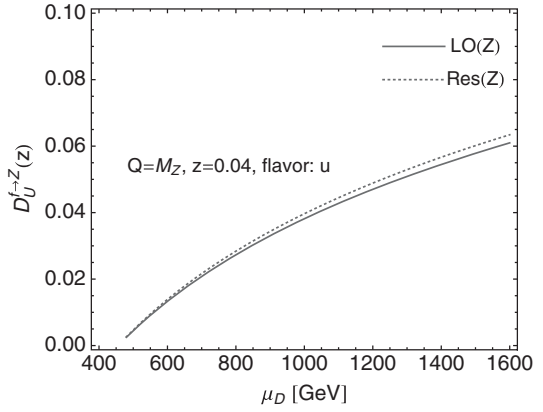

FIG. 4. Evolution of the LO and resummed fragmentation functions for a u quark into a Z boson with momentum fraction $z = 0.04$.

and renormalization scales, as well as the fragmentation scale, equal to the transverse mass $m_T = \sqrt{Q^2 + p_T^2}$, unless specified otherwise. The scale dependence of our numerical results is discussed later. As shown in Fig. 5, the cross sections decrease quickly with increasing p_T at the LHC, caused by the fast drop of the partonic flux at large partonic momentum fraction x. With a larger phase space available at the 100 TeV collider, the p_T spectrum decreases more slowly. The NLO QCD corrections can be as large as 50% of the LO cross sections for the LHC energies and reach 60% for the 100 TeV collider.

To quantify the size of contributions from the large fragmentation logarithms, we compare the full NLO corrections with the part of the corrections proportional to the fragmentation logarithms, equal to the fragmentation contribution in Eq. (8) expanded to the same order in α_s. In Fig. 6, we plot the normalized full NLO corrections,

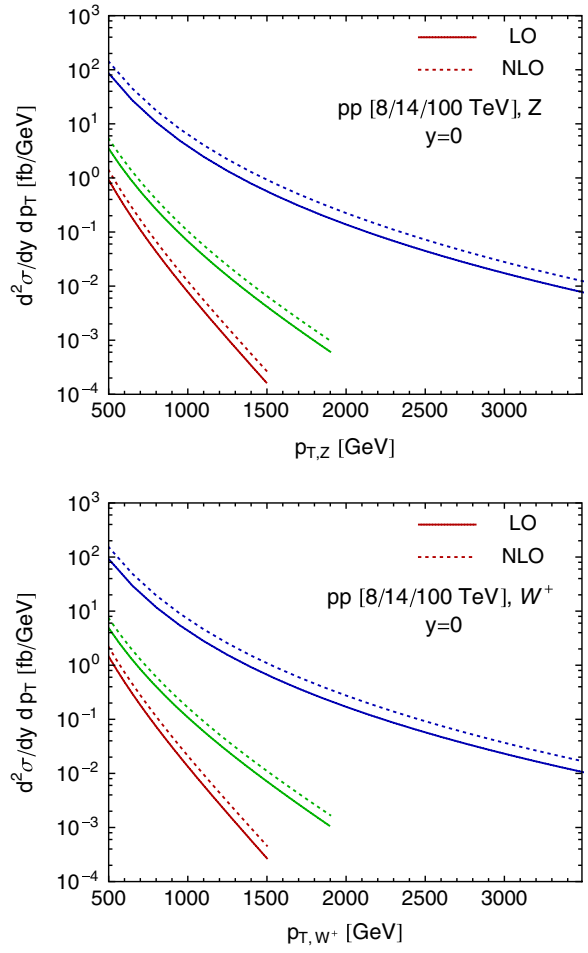

FIG. 5 (color online). The LO and NLO predictions for the double-differential cross sections of Z and W^+ boson production at large transverse momentum, p_T, in the conventional fixed-order perturbative expansion, at $\sqrt{s} = 8$ and 14 TeV at the LHC and 100 TeV at a future proton-proton collider. The range of p_T is determined by the available phase space of the collisions.

$R_{\rm cor} = (\sigma^{\rm NLO} - \sigma^{\rm LO})/\sigma^{\rm LO}$ (solid lines), along with the normalized contributions proportional to the fragmentation logarithms (dashed lines). The full NLO corrections are large and increase quickly for vector-boson production at the LHC as p_T approaches its maximum. The behavior differs slightly for different vector bosons owing to the different masses and different contributing PDFs. The fragmentation pieces contribute about one-third of the full NLO corrections for the p_T values considered. With the larger phase space available for radiation, the NLO fragmentation contributions are more significant at the 100 TeV collider. Their magnitude is as large as 30% of the LO cross sections or about one-half of the full NLO corrections. The fragmentation contributions are almost insensitive to the value of p_T for the 100 TeV collider, and they stay pretty much constant when $p_T \gtrsim 1$ TeV for both W and Z bosons. This result comes about because the logarithmic enhancements from $\ln(p_T/Q)$ are also modulated by the z dependence of the hard partonic cross sections in the convolution with the fragmentation functions.

Equation (8) expresses the fragmentation contribution as a convolution of two PDFs and one fragmentation function, and the hard scale of the partonic scattering is proportional to the combination x_1x_2/z. The factored fragmentation contribution should likely be dominated by the kinematic region where x_1 and x_2 are small, while z is relatively large, owing to the competition of two steeply falling PDFs against one fragmentation function when the momentum fractions, x or z, increase. To better understand the dominant region of partonic scattering, we introduce a cutoff, $z_{\rm cut} \leq 1$, to limit the z-integration in Eq. (8) to $z_{\rm min} \leq z \leq z_{\rm cut}$, instead of $z_{\rm min} \leq z \leq 1$. In Fig. 7, we plot $\sigma^{\rm F\text{-}LO}$ for Z boson production as a function of the cutoff, $z_{\rm cut}$, normalized by the full contribution with $z_{\rm cut} = 1$, to show the fractional contributions from a limited phase space in z. As expected, the contributions at large z dominate in the fragmentation pieces. For example, the domain $z > 0.5$ contributes over 90% of the fragmentation

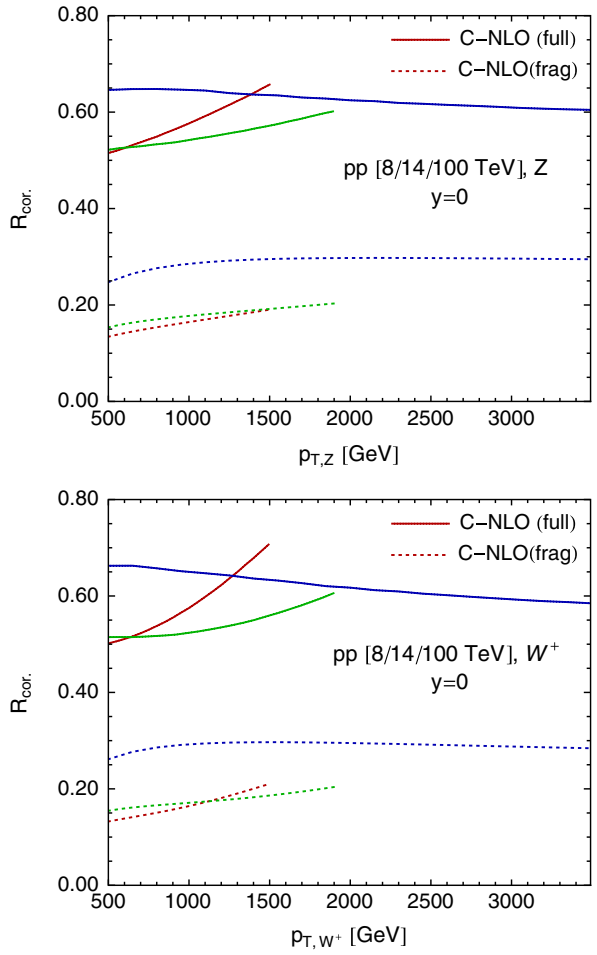

FIG. 6 (color online). The full NLO corrections in the conventional fixed-order expansion scheme and the corresponding contributions proportional to the fragmentation logarithms, both normalized to the conventional LO cross sections, are plotted as a function of p_T for Z and W^+ boson production in proton-proton collisions at $\sqrt{s} = 8$, 14 and 100 TeV.

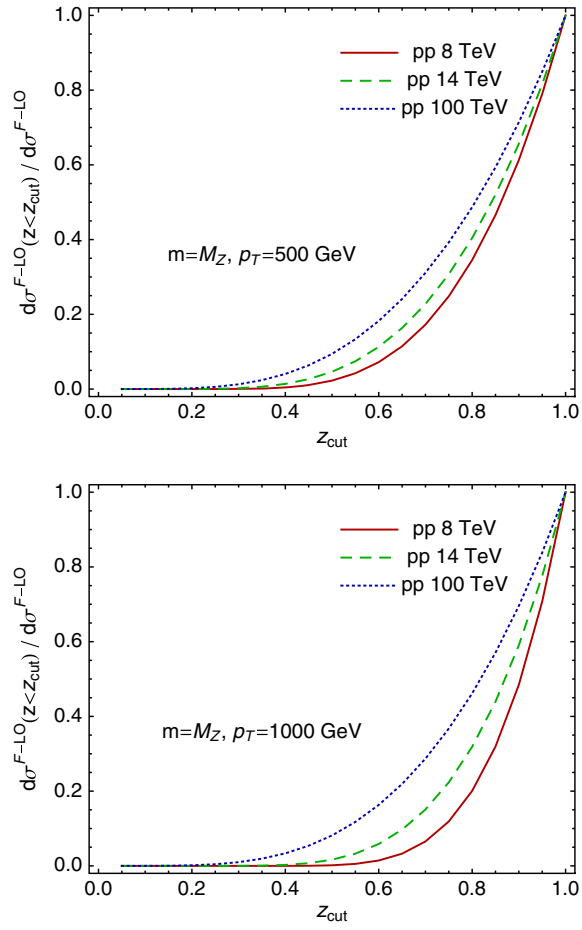

FIG. 7 (color online). Fractional contribution of $\sigma^{\rm F\text{-}LO}$ for Z boson production as a function of the cutoff, $z_{\rm cut}$, of the upper limit of z-integration in Eq. (8), at $p_T = 500$ and 1000 GeV and $y = 0$.

cross sections for all collision energies shown in Fig. 7. The effective range of z is even more limited to the larger z-values for production at the LHC energies owing to the smaller phase space for a given p_T.

In Fig. 8, we plot the LO and NLO contributions to the double-differential cross sections of Z boson production at $y = 0$, evaluated in the conventional fixed-order perturbative expansion and normalized by the conventional LO cross sections. The uncertainty bands in Fig. 8 are calculated by varying the renormalization and factorization scales, $\mu_r = \mu_f = \mu$, upward and downward by a factor of 2, as an estimation of the remaining higher-order contributions. There are moderate reductions of the scale variation from LO to NLO for the LHC energy, while the LO result at the 100 TeV collider shows a scale variation that is too small due to accidental cancellations between the renormalization and the factorization scale dependence. One may also notice that the NLO bands do not overlap the LO bands, suggestive that the scale variations for the conventional fixed-order perturbative expansion may underestimate the true theoretical uncertainties from the remaining high-order corrections.

C. W and Z boson production at large p_T in the modified expansion scheme

In our modified factorization scheme, we split the conventional fixed-order perturbative series into the direct and fragmentation contributions, as shown in Eq. (7), and we calculate them to NLO in this paper. In Fig. 9, we plot both the LO and NLO direct contributions to the double-differential cross sections of Z boson production. The results are presented as a ratio R_μ, normalized by the conventional LO cross sections. Note that, as mentioned earlier, the direct contribution at LO equals the conventional LO cross section. Similarly, in Fig. 10, we plot the corresponding LO and NLO fragmentation contributions, normalized by the same conventional LO cross sections. In our modified factorization scheme, there is a fragmentation scale μ_D, in addition to the renormalization scale μ_r and

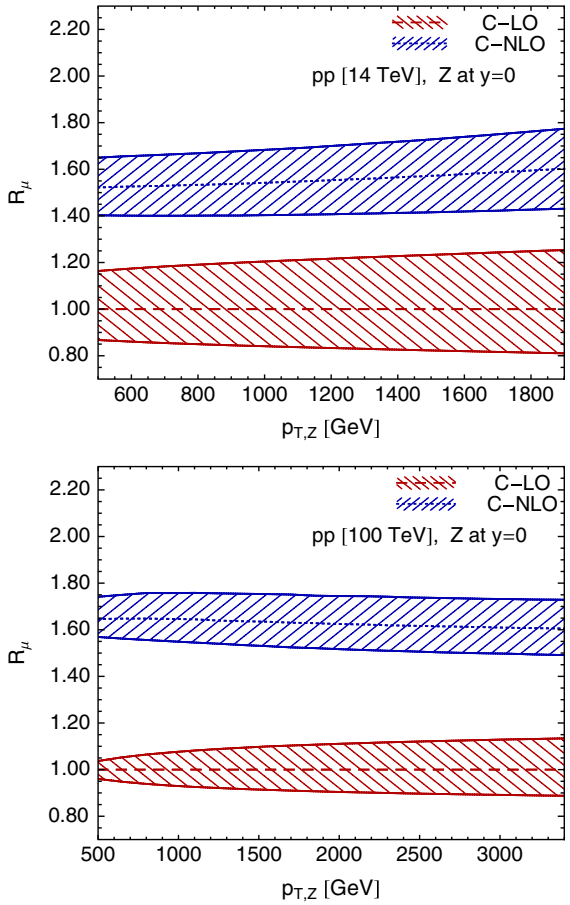

FIG. 8 (color online). Conventional LO and NLO predictions on double-differential cross sections of Z boson production at 14 and 100 TeV, including the central predictions and the scale variations, all normalized to the central predictions of the conventional LO results.

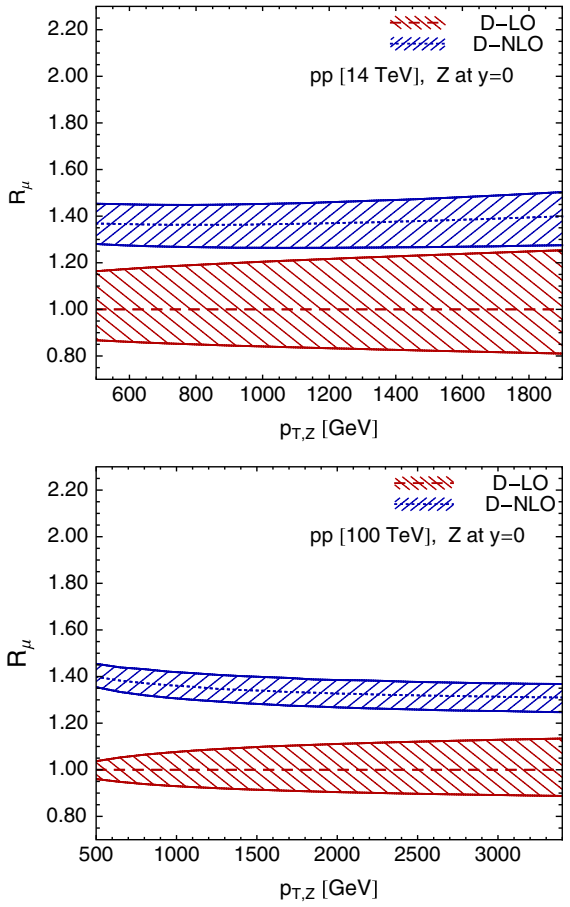

FIG. 9 (color online). LO and NLO predictions for the direct contributions to double-differential cross sections of Z boson production in proton-proton collisions at $\sqrt{s} = 14$ and 100 TeV, respectively, with uncertainty bands from the scale variations. The predictions are normalized by the central values of the conventional LO cross sections.

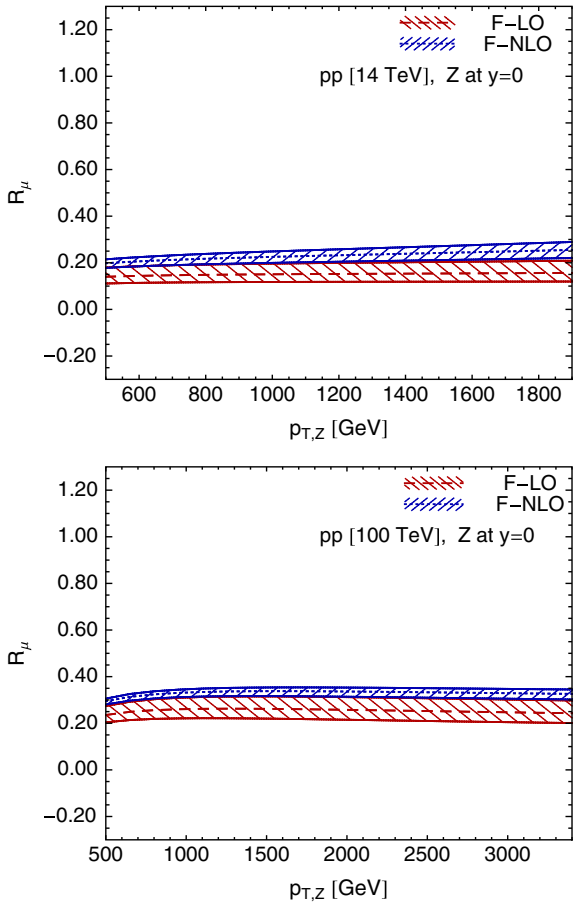

FIG. 10 (color online). LO and NLO predictions for the fragmentation contributions to double-differential cross sections of Z boson production in proton-proton collisions at $\sqrt{s} = 14$ and 100 TeV, respectively, with uncertainty bands from the scale variations. The predictions are normalized by the central values of the conventional LO cross sections.

factorization scale μ_f, which are the same as those in the conventional fixed-order factorization scheme. Different choices of μ_D effectively move some finite perturbative contributions between the direct and the fragmentation contributions in Eq. (7). We set the default choice for all three scales equal to m_T. The uncertainty bands in Figs. 9 and 10 are calculated by varying the renormalization and factorization scales, $\mu_r = \mu_f = \mu$, upward and downward by a factor of 2, as an estimation of the remaining higher-order contributions. The effects from varying the fragmentation scale, μ_D, are discussed later.

Comparing the relative size of NLO corrections in our modified factorization scheme with those of the conventional fixed-order expansion, we see in Figs. 8, 9, and 10 that the NLO K-factors in the conventional expansion are significantly larger than those evaluated in the modified scheme. The improved convergence of our modified expansion scheme indicates a better control of unknown higher-order corrections. In Fig. 10, we observe significant reduction of the scale variation for the fragmentation contributions at NLO as a consequence of the inclusion of the NLO partonic hard parts.

As expressed in Eq. (7), the full NLO predictions in our modified factorization scheme are equal to the sum of the NLO direct and fragmentation contributions. They differ from the conventional NLO results by additional higher-order contributions, or the type-B corrections, defined in Eq. (10). In Fig. 11, we plot the full NLO predictions in our modified factorization scheme for the double-differential cross sections of Z boson production, together with the conventional NLO results, where we show both the central predictions and the scale variation. Both are normalized by the central values of the conventional LO cross sections. Note that the scale-variation (blue) band of the modified factorization scheme lies almost entirely within the (red) band of the conventional scheme. At NLO accuracy, the predictions from the conventional fixed-order perturbative expansion show about 20% uncertainty from the scale

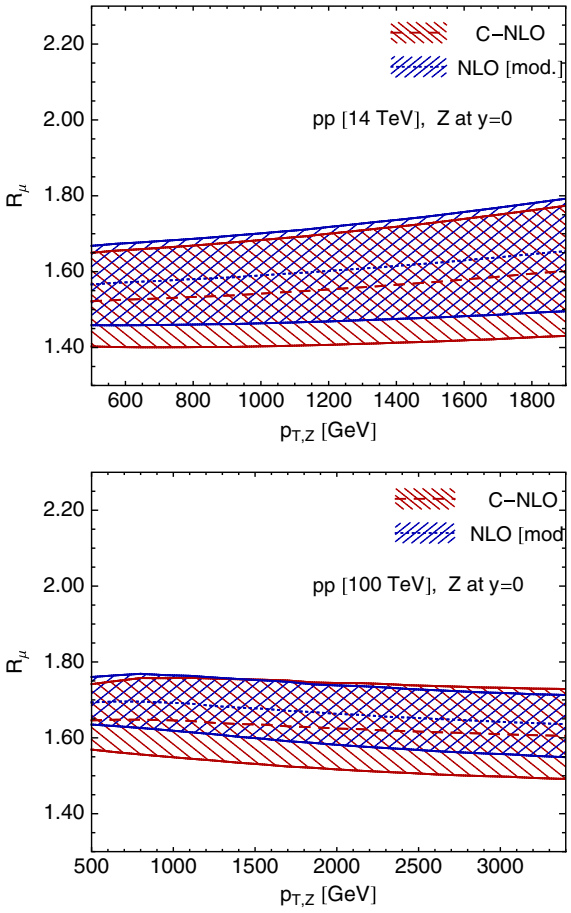

FIG. 11 (color online). The full NLO predictions in the modified factorization scheme for double-differential cross sections of Z boson production at 14 and 100 TeV, including the central predictions and the scale variations, together with the conventional NLO results, all normalized to the central predictions of the conventional LO results.

variation, which increases with p_T, while, as expected, the full NLO predictions from our modified factorization scheme show a reduction of the uncertainty, because of the inclusion of the type-B corrections. The reduction is stronger for the NLO predictions at $\sqrt{s} = 100$ TeV, where the fragmentation contributions are significantly larger, as shown in Fig. 6.

The central values of the NLO predictions from our modified factorization scheme are larger than the NLO predictions from the conventional factorization scheme, as shown in Fig. 11. This result is an immediate consequence of the type-B corrections in Eq. (10). To further quantify this difference, we plot the type-B corrections for both the Z and W^+ boson production in Fig. 12, along with the type-A corrections, as specified in the discussion immediately after Eq. (11). Both type-A and type-B corrections in Fig. 12 are shown as ratios to the conventional LO cross sections, $R_{\rm cor} = (\sigma^{\rm D\text{-}NLO} + \sigma^{\rm F\text{-}NLO} - \sigma^{\rm C\text{-}NLO})/\sigma^{\rm C\text{-}LO}$. Unlike the type-B corrections, which are positive and

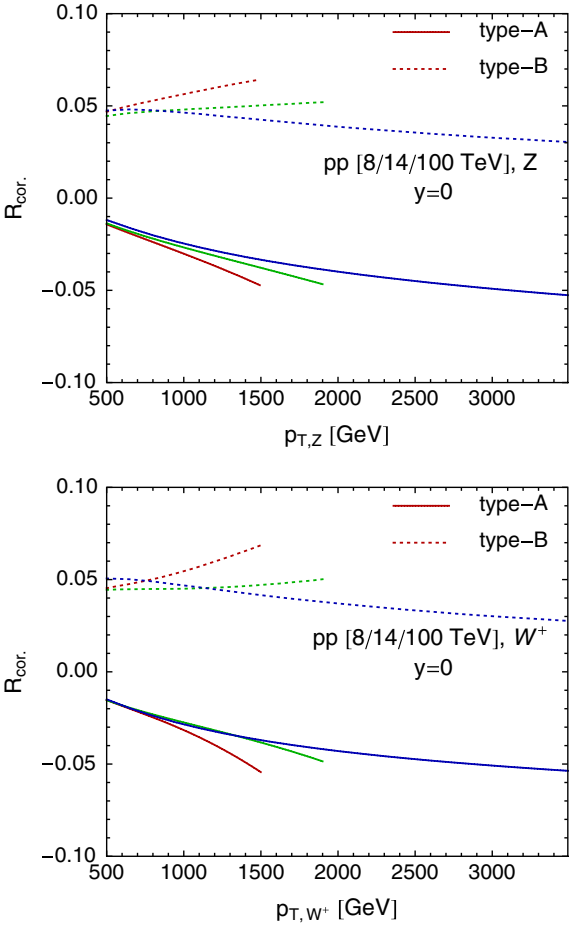

FIG. 12 (color online). Differences between the full NLO predictions in the modified factorization scheme and the conventional NLO predictions, for double-differential cross sections of Z and W^+ boson production at 8, 14, and 100 TeV, in each subfigure with increasing range of p_T.

defined to be the total corrections at NLO, the type-A corrections are negative and are of a few percent of the LO cross sections. As shown in Eq. (10), the type-A corrections are proportional to the difference between the fully resummed and the LO perturbative fragmentation functions. The fully resummed fragmentation functions have a softer z dependence when compared to the LO piece of the functions, and naturally the difference is negative for the large z region, while it becomes positive and larger as z decreases, as shown in Fig. 3. The negative type-A corrections, as shown in Fig. 12, arise from the fact that the fragmentation contributions are dominated by the large z region, as discussed above. Numerically, the type-A corrections are within -6% for all cases shown in Fig. 12, similar to the results for virtual photon production [47]. At a given p_T, the absolute size of the corrections is larger for production at a lower $\sqrt{s}$ owing to the smaller phase space for radiation and larger effective z values. The net type-B corrections are positive, despite the negative type-A corrections, because the fragmentation corrections from NLO hard matrix elements are positive, bringing the total corrections up by 6%–10%. This outcome is understandable since the NLO corrections to parton or jet production at hadron colliders, which share the similar hard matrix elements, are usually positive and large.

As shown in Fig. 12, the final numerical differences between the NLO predictions, calculated in our modified factorization scheme, and the conventional fixed-order perturbative expansion are about 5% at $p_T = 500$ GeV and increase or decrease slightly for the case of the LHC or a 100 TeV proton-proton collider. The corrections are similar for Z and W^+ boson production. Based on the relatively weak p_T dependence of the corrections in Fig. 12, we expect that the NLO predictions from our modified factorization scheme will not differ appreciably for the overall shape of the large p_T spectrum of the W or Z at the LHC derived from the conventional NLO calculations. At the 100 TeV proton-proton collider, our NLO predictions for the large p_T spectrum of both the W and Z boson production could be slightly softer than the NLO spectrum evaluated from conventional fixed-order perturbative calculations without resummation of the fragmentation logarithms. It is the resummation of the large fragmentation logarithms that makes our modified factorization formalism more stable and converge faster perturbatively.

To examine the fragmentation scale dependence of the NLO predictions of our modified factorization scheme, we increased and decreased the scale by a factor of 2 from its default value, $\mu_D = m_T$, while fixing the renormalization and factorization scales. Our NLO results in the modified factorization scheme show a very weak dependence on μ_D, at a level of 1%. By comparing the fragmentation scale dependence between the direct and the fragmentation contribution to the production cross sections, $\sigma^{\rm D}$ and $\sigma^{\rm F}$ in Eq. (7), we observe that the leading dependence on μ_D

in σ^{F} cancels that in σ^{D} by definition. The subleading dependence on μ_D from QCD evolution cancels within σ^{F} between the resummed corrections to the fragmentation functions and the NLO corrections to hard matrix elements. Thus, the remaining dependence on μ_D in the sum of $\sigma^{\mathrm{D\text{-}NLO}}$ and $\sigma^{\mathrm{F\text{-}NLO}}$ is negligible.

In conclusion, within the modified factorization scheme, we split vector-boson production at large p_T into two separate perturbation series, both of which show better convergence compared to the conventional fixed-order calculations. By including some higher-order corrections (beyond NLO in conventional fixed order) for the fragmentation contributions, we reduce the scale variations and obtain a perturbative expansion with better control of the theoretical uncertainties, especially for vector-boson production at the 100 TeV collider.

D. Discussion of the numerical results

In Table I we summarize our total cross sections for vector-boson production, integrated over the full rapidity range, with $p_{T,V}$ greater than 800 GeV. We provide predictions based on conventional LO and NLO in the second and third columns and the NLO predictions using the modified factorization scheme in the last column, for the LHC at 13 TeV and for a future proton-proton collider at 100 TeV. We choose a p_T threshold of 800 GeV for illustration. As shown in Table I, the total cross section for Z boson production at $\sqrt{s} = 13$ TeV can reach 120 fb with a scale uncertainty about $\pm 8\%$. The scale uncertainty is about $\pm 5\%$ for Z boson production at the 100 TeV collider. Uncertainties due to variations of the fragmentation scale μ_D are not included since they are much smaller. These residual scale variations should be further reduced either by soft gluon resummation [34–41] or ongoing NNLO calculations. Other uncertainties include PDF uncertainties of about $\pm 4\%$ for Z or W boson production at 13 TeV and about $\pm 1\%$ for the 100 TeV collider, obtained using the META PDF prescription proposed in [58]. The PDF uncertainties are much larger at 13 TeV because the large-x region of the PDFs is being probed, a situation that could be improved once more LHC data are included in the global analysis of PDFs. For vector-boson production at large p_T at the LHC, the electroweak corrections due to Sudakov logarithms are also significant [11–18] and must be included when comparison is made with data.

TABLE I. Cross sections integrated over y and $p_T > 800$ GeV with scale variations, for W and Z boson production at 13 TeV (in fb) and at 100 TeV (in pb). The scale uncertainties are calculated by varying $\mu_r = \mu_f = \mu$ by a factor of 2 in both directions around m_T. The uncertainties due to variations of μ_D are not included since they are much smaller.

$\sigma_{p_T>800\ \mathrm{GeV}}$	VB	C-LO	C-NLO	NLO [modified]
13 TeV [fb]	Z	74.1	$117.4^{+12.0}_{-11.5}$	$120.5^{+9.2}_{-10.4}$
	W^+	126.2	$199.4^{+20.1}_{-19.3}$	$204.4^{+15.4}_{-17.3}$
	W^-	55.8	$90.2^{+9.6}_{-9.2}$	$92.7^{+7.4}_{-8.2}$
100 TeV [pb]	Z	11.48	$19.68^{+1.53}_{-1.30}$	$20.16^{+1.00}_{-0.98}$
	W^+	15.08	$26.23^{+2.14}_{-1.79}$	$26.86^{+1.41}_{-1.35}$
	W^-	10.50	$18.18^{+1.47}_{-1.23}$	$18.61^{+0.96}_{-0.92}$

Measurements exist at $\sqrt{s} = 7$ TeV at the LHC of the Z boson p_T spectrum in the leptonic channel [6] and of the Z or W boson cross sections above a certain p_T threshold in the hadronic channel [7]. The highest effective p_T of the vector boson is limited to about 300 GeV. At 13 TeV, according to Table I, ~2400 Z bosons are expected with p_T above 800 GeV in the dimuon and dielectron channel, assuming an integrated luminosity of 300 fb^{-1}. The statistical uncertainties are estimated to be smaller than the scale variations in Table I. Thus, precise tests of various QCD predictions require good control of the experimental systematical uncertainties at 13 and 100 TeV. The situation is similar for W boson production where we gain a larger branching ratio in the leptonic channel but suffer from lower efficiency in the event reconstruction.

IV. SUMMARY

We introduced a modified factorization scheme for evaluating the transverse momentum spectrum of the SM W and Z boson production at hadron colliders. In this new scheme, we reorganize the conventional fixed-order QCD perturbative expansion into two separate perturbative expansions, corresponding to direct and fragmentation contributions. The fragmentation piece has a typical two-stage pattern, production of an on-shell parton convoluted with the perturbative fragmentation functions of the W and Z boson, as illustrated in Fig. 1. When $p_T^2 \gg Q^2$, the large perturbative fragmentation logarithms of $\ln(p_T^2/Q^2)$ are resummed into the fragmentation functions by solving their evolution equations. Consequently, the short-distance partonic hard parts for both the direct and the fragmentation contributions are free of these large fragmentation logarithms, and the overall convergence of the reorganized perturbative expansions is improved, in particular, for the region where $p_T^2 \gg Q^2$.

In our explicit NLO calculations, the fragmentation logarithms make up a large portion of the conventional NLO K-factors at high p_T at the LHC and especially at a future 100 TeV collider. Our improved NLO predictions retain all ingredients in the conventional NLO calculations [up to $\mathcal{O}(\alpha_{em}\alpha_s^2)$], but they include partial higher-order corrections. In comparison with the conventional fixed-order perturbative expansion, the modified NLO predictions show a moderate reduction of the scale variation at large p_T and improved convergence. The improved NLO predictions are about 5% higher in the normalization of the

large-p_T spectrum, but they provide only modest changes in the shape of the spectrum. In subsequent research, it would be desirable to extend the analysis to NNLO. Our modified factorization scheme could be applied to the production of other heavy particles, such as the Higgs boson and top quark, at large p_T when the p_T of the produced state is much larger than its mass.

ACKNOWLEDGMENTS

The research of E. L. B. and J. G. in the High Energy Physics Division at Argonne is supported by the US Department of Energy, High Energy Physics, Office of Science, under Contract No. DE-AC02-06CH11357. The research of Z. B. K. is partially supported by the US Department of Energy, Office of Science, under Contract No. DE-AC52-06NA25396. The research of J. W. Q. is supported in part by the US Department of Energy under Contract No. DE-AC02-98CH10886 and the National Science Foundation under Grants No. PHY-0969739 and No. PHY-1316617. H. Z. is supported by the US DOE under Contracts No. DE-FG02-91ER40618 and No. DE-SC0011702.

[1] G. Aad *et al.* (ATLAS Collaboration), Phys. Lett. B **716**, 1 (2012).
[2] S. Chatrchyan *et al.* (CMS Collaboration), Phys. Lett. B **716**, 30 (2012).
[3] E. L. Berger, F. Halzen, C. S. Kim, and S. Willenbrock, Phys. Rev. D **40**, 83 (1989); **40**, 3789 (1989)].
[4] C. S. Kim, A. D. Martin, and W. J. Stirling, Phys. Rev. D **42**, 952 (1990).
[5] S. A. Malik and G. Watt, J. High Energy Phys. 02 (2014) 025.
[6] G. Aad *et al.* (ATLAS Collaboration), J. High Energy Phys. 09 (2014) 145.
[7] G. Aad *et al.* (ATLAS Collaboration), New J. Phys. **16**, 113013 (2014).
[8] R. J. Gonsalves, J. Pawlowski, and C. F. Wai, Phys. Rev. D **40**, 2245 (1989).
[9] H. Baer and M. H. Reno, Phys. Rev. D **44**, R3375 (1991).
[10] P. B. Arnold and R. P. Kauffman, Nucl. Phys. **B349**, 381 (1991).
[11] E. Maina, S. Moretti, and D. A. Ross, Phys. Lett. B **593**, 143 (2004); **614**, 216 (2005)].
[12] J. H. Kuhn, A. Kulesza, S. Pozzorini, and M. Schulze, Phys. Lett. B **609**, 277 (2005).
[13] J. H. Kuhn, A. Kulesza, S. Pozzorini, and M. Schulze, Nucl. Phys. **B727**, 368 (2005).
[14] W. Hollik, T. Kasprzik, and B. A. Kniehl, Nucl. Phys. **B790**, 138 (2008).
[15] J. H. Kuhn, A. Kulesza, S. Pozzorini, and M. Schulze, Phys. Lett. B **651**, 160 (2007).
[16] J. H. Kuhn, A. Kulesza, S. Pozzorini, and M. Schulze, Nucl. Phys. **B797**, 27 (2008).
[17] T. Becher and X. Garcia i Tormo, Phys. Rev. D **88**, 013009 (2013).
[18] S. Kallweit, J. M. Lindert, P. Maierhfer, S. Pozzorini, and M. Schnherr, J. High Energy Phys. 04 (2015) 012.
[19] J. C. Collins, D. E. Soper, and G. F. Sterman, Nucl. Phys. **B250**, 199 (1985).
[20] C. T. H. Davies and W. J. Stirling, Nucl. Phys. **B244**, 337 (1984).
[21] C. Balazs and C. P. Yuan, Phys. Rev. D **56**, 5558 (1997).
[22] R. K. Ellis and S. Veseli, Nucl. Phys. **B511**, 649 (1998).
[23] J. W. Qiu and X. f. Zhang, Phys. Rev. Lett. **86**, 2724 (2001).
[24] J. W. Qiu and X. f. Zhang, Phys. Rev. D **63**, 114011 (2001).
[25] E. L. Berger and J. W. Qiu, Phys. Rev. D **67**, 034026 (2003).
[26] F. Landry, R. Brock, P. M. Nadolsky, and C. P. Yuan, Phys. Rev. D **67**, 073016 (2003).
[27] S. Mantry and F. Petriello, Phys. Rev. D **83**, 053007 (2011).
[28] T. Becher and M. Neubert, Eur. Phys. J. C **71**, 1665 (2011).
[29] G. Bozzi, S. Catani, G. Ferrera, D. de Florian, and M. Grazzini, Phys. Lett. B **696**, 207 (2011).
[30] S. Mantry and F. Petriello, Phys. Rev. D **84**, 014030 (2011).
[31] T. Becher, M. Neubert, and D. Wilhelm, J. High Energy Phys. 02 (2012) 124.
[32] S. Catani, L. Cieri, D. de Florian, G. Ferrera, and M. Grazzini, Nucl. Phys. **B881**, 414 (2014).
[33] Y. Wang, C. S. Li, Z. L. Liu, D. Y. Shao, and H. T. Li, Phys. Rev. D **88**, 114017 (2013).
[34] N. Kidonakis and V. Del Duca, Phys. Lett. B **480**, 87 (2000).
[35] N. Kidonakis and A. Sabio Vera, J. High Energy Phys. 02 (2004) 027.
[36] R. J. Gonsalves, N. Kidonakis, and A. Sabio Vera, Phys. Rev. Lett. **95**, 222001 (2005).
[37] T. Becher, C. Lorentzen, and M. D. Schwartz, Phys. Rev. Lett. **108**, 012001 (2012).
[38] N. Kidonakis and R. J. Gonsalves, Phys. Rev. D **87**, 014001 (2013).
[39] T. Becher, C. Lorentzen, and M. D. Schwartz, Phys. Rev. D **86**, 054026 (2012).
[40] T. Becher, G. Bell, C. Lorentzen, and S. Marti, J. High Energy Phys. 02 (2014) 004.
[41] N. Kidonakis and R. J. Gonsalves, Phys. Rev. D **89**, 094022 (2014).
[42] R. Boughezal, F. Caola, K. Melnikov, F. Petriello, and M. Schulze, J. High Energy Phys. 06 (2013) 072.
[43] X. Chen, T. Gehrmann, E. W. N. Glover, and M. Jaquier, Phys. Lett. B **740**, 147 (2015).
[44] R. Boughezal, C. Focke, X. Liu, and F. Petriello, arXiv: 1504.02131.
[45] M. Rubin, G. P. Salam, and S. Sapeta, J. High Energy Phys. 09 (2010) 084.
[46] E. L. Berger, L. E. Gordon, and M. Klasen, Phys. Rev. D **58**, 074012 (1998).

[47] E. L. Berger, J. W. Qiu, and X. f. Zhang, Phys. Rev. D **65**, 034006 (2002).
[48] Z. B. Kang, J. W. Qiu, and W. Vogelsang, Phys. Rev. D **79**, 054007 (2009).
[49] Y. Q. Ma, J. W. Qiu, G. Sterman, and H. Zhang, Phys. Rev. Lett. **113**, 142002 (2014).
[50] Y. I. Azimov, Y. L. Dokshitzer, and V. A. Khoze, Yad. Fiz. **36**, 1510 (1982) [Sov. J. Nucl. Phys. **36**, 878 (1982)]; Y. I. Azimov, Y. L. Dokshitzer, V. A. Khoze, and S. I. Troian, Yad. Fiz. **40**, 777 (1984) [Sov. J. Nucl. Phys. **40**, 498 (1984)]; Y. L. Dokshitzer, V. A. Khoze, and S. I. Troian, J. Phys. G **17**, 1481 (1991).
[51] J. C. Collins, D. E. Soper, and G. F. Sterman, Adv. Ser. Dir. High Energy Phys. **5**, 1 (1988).
[52] J. W. Qiu and X. f. Zhang, Phys. Rev. D **64**, 074007 (2001).
[53] F. Aversa, P. Chiappetta, M. Greco, and J. Guillet, Nucl. Phys. **B327**, 105 (1989).
[54] J. C. Collins and J. W. Qiu, Phys. Rev. D **39**, 1398 (1989).
[55] E. Braaten and J. Lee, Phys. Rev. D **65**, 034005 (2002).
[56] A. Denner and T. Sack, Nucl. Phys. **B358**, 46 (1991).
[57] J. Beringer *et al.* (Particle Data Group Collaboration), Phys. Rev. D **86**, 010001 (2012).
[58] J. Gao and P. Nadolsky, J. High Energy Phys. 07 (2014) 035.
[59] J. Gao, M. Guzzi, J. Huston, H.-L. Lai, Z. Li, P. Nadolsky, J. Pumplin, D. Stump, and C.-P. Yuan, Phys. Rev. D **89**, 033009 (2014).
[60] A. D. Martin, W. J. Stirling, R. S. Thorne, and G. Watt, Eur. Phys. J. C **63**, 189 (2009).
[61] R. D. Ball *et al.*, Nucl. Phys. **B867**, 244 (2013).